

# INCLUSION BY A FLUORENYL DIOL HOST WITH SUBSTITUTED PYRIDINES

## Structures, selectivity and kinetics of desorption

L. R. Nassimbeni<sup>1</sup>, G. Ramon<sup>1\*</sup> and E. Weber<sup>2</sup>

<sup>1</sup>Department of Chemistry, University of Cape Town, Rondebosch 7701, South Africa

<sup>2</sup>Institut für Organische Chemie, Technische Universität Bergakademie Freiberg, Leipziger Strasse 29, 09596 Freiberg/Sachs, Germany

The structures of the inclusion compounds formed by the host 9,9'-(ethyne-1,2-diyl)bis(fluoren-9-ol) with pyridine and picolines are similar and display tubular topology. The host discriminates poorly between these guests. The kinetics of desorption of the pyridine compound is governed by the Avrami–Erofe'ev equation A2, with an activation energy of 111(7) kJ mol<sup>-1</sup>.

**Keywords:** desorption kinetics, inclusion compound, selectivity

### Introduction

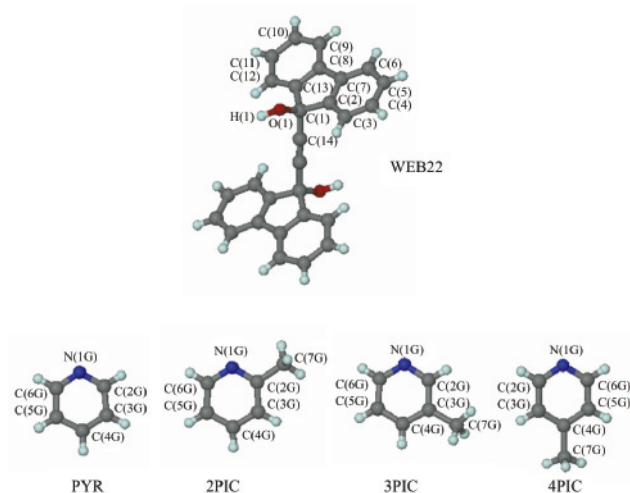
The essence of supramolecular chemistry is the non-covalent bond, and an understanding of intermolecular forces, their strengths, directions, and their role in the process of molecular self assembly, is crucial to the study of inclusion compounds. Crystalline clathrates, made up of host and guest components, are appropriate systems to study these non-bonded interactions, because one can attempt to correlate their structures with their reactivity, their thermal stability and their kinetics of decomposition and formation.

Fluorenyl host compounds have been studied extensively, as they have the capacity to enclathrate a variety of guest molecules [1]. They conform to Weber's host design specifications, being rigid, bulky, and if they contain the hydroxyl moiety, they

are likely to form coordinato-clathrates via hydrogen bonding [2].

A series of these compounds containing hydroxyfluorenyl groups separated by spacers have been synthesized and their enclathrating properties have been explored [3]. They correspond to the general design of 'wheel and axle' molecules, of which 1,1,6,6-tetraphenylhexa-2,4-diyne-1,6-diol is the best exemplar [4], and which has been studied extensively [5].

The host 9,9'-(ethyne-1,2-diyl)bis(fluoren-9-ol) forms inclusion compounds with a variety of guests including aliphatic amines, aliphatic alcohols, DMSO, 1,4-dioxane and benzene, and its structures with 1-propanol, cyclohexanol and THF have been elucidated [3].



**Scheme 1** Numbering of the host and guest molecules

\* Author for correspondence: gaelle.ramon@uct.ac.za

We now present our results on the structural characterization of the inclusion compounds formed by this host with pyridine and the picoline isomers, as well as their thermal stabilities, selectivity profiles and kinetics of desorption. The atomic numbering scheme is given in Scheme 1.

## Experimental

### *Crystal structures*

Crystals of the inclusion compounds were obtained by crystallising saturated solutions of the host WEB22 in the respective guests, giving rise to: WEB22·2(2PIC), WEB22·2(3PIC), WEB22·2(4PIC) and WEB22·2PYR at 25°C.

In all cases the host-guest ratios were confirmed by thermogravimetry (TG) and details of the crystal data, intensity data collections and refinements are contained in Table 1. Cell dimensions were established from the intensity data measurements on a Nonius Kappa CCD diffractometer using graphite-monochromated MoK $_{\alpha}$  radiation. The strategy for the data collections was evaluated using COLLECT software [6]. For all structures, data were collected by the standard phi- and omega-scan techniques, and were scaled and reduced using DENZO-SMN software [7]. The structures were solved by direct methods using SHELX-86 [8] and refined by least squares with SHELX-97 [9] refining on  $F^2$ . The program X-Seed [10, 11] was used as a graphical interface for the structure solution and refinement using SHELX, as well as to produce the packing diagrams.

The direct methods yielded the positions of the non-hydrogen atoms. Hydroxyl hydrogen atoms were located in difference electron density maps and refined independently with simple bond length constraints and independent temperature factors. The other hydrogen atoms were placed with geometric constraints and assigned isotropic temperature factors of  $1.2U_{eq}$  of their parent atoms. All non-hydrogen atoms were refined with anisotropic temperature factors. All structures were determined at low temperature (113 K).

### *Thermal analysis*

Differential scanning calorimetry (DSC) was performed on a PerkinElmer PC7 series system and thermogravimetry (TG) on a Mettler Toledo TGA/SDTA 851<sup>c</sup> system. Finely powdered, air-dried specimens (2–5 mg) were placed in crimped, vented aluminium DSC pans or open aluminium TG sample pans. Dinitrogen was used as purging gas at a flow rate of 30 mL min<sup>-1</sup>. All experiments were car-

ried out over temperature ranges of 30–300°C for DSC and 30–350°C for the TG experiments at a constant heating rate of 20°C min<sup>-1</sup>.

### *Kinetics of desolvation*

The kinetics of desolvation of WEB22·2(2PIC) were studied by carrying out a series of isothermal TG runs, performed over the temperature range 333–363 K taking readings at intervals of 10 K. The mass loss data were converted to extent of reaction ( $\alpha$ ) vs. time curves, which were fitted by trial and error to various kinetic laws [12],  $\alpha$  being:

$$\alpha = \frac{m_0 - m_t}{m_0 - m_{\infty}}$$

where  $m_0$ ,  $m_t$  and  $m_{\infty}$  are the recorded masses at the start, during and end of the experiment.

### *Competition experiments*

Two-component competition experiments were studied but because of the very similar boiling points of 3-picoline and 4-picoline (respectively 144 and 145°C), the GC did not allow to study this combination as the peaks could not be separated. All the other possible two-component combinations between the guests were studied and were extended to three-component competition experiments.

In the case of 2-component competition, the mixtures of the two guests were prepared in vials in which the mole fraction of a given guest varied from 0 to 1 in steps of 0.1. A fixed amount of host compound was added and dissolved by heating and stirring. The ratio of the host compound to the total guest was at least 1:20 to ensure that there was enough of the guest of lower mole fraction should the host have 100% preference for it.

In the case of 3-component competition, the mixtures prepared were represented on an equilateral triangle whose apices represent the pure guest compounds. The starting mixture compositions were defined from an inner equilateral triangle as well as from the centre of the triangle, which represents the equimolar mixture of the guests (0.33 mol fraction for each).

The resulting crystals were removed from the mother liquor and dried over filter paper. They were placed in airtight glass vials with silicone seals incorporated into a screw-on lid while being dissolved in a minimum amount of acetone. These solutions as well as the starting solutions were analysed by gas chromatography (GC).

These analyses were carried out using a Varian 3900 gas chromatograph connected to a computer and equipped with a CP-1177 split/splitless in-

Table 1 Crystal data and refinement parameters

	WEB22-2(PYR)	WEB22-2(2PIC)	WEB22-2(3PIC)	WEB22-2(4PIC)
Molecular formula	C <sub>28</sub> H <sub>18</sub> O <sub>2</sub> ·2(C <sub>5</sub> H <sub>5</sub> N)	C <sub>28</sub> H <sub>18</sub> O <sub>2</sub> ·2(C <sub>6</sub> H <sub>7</sub> N)	C <sub>28</sub> H <sub>18</sub> O <sub>2</sub> ·2(C <sub>6</sub> H <sub>7</sub> N)	C <sub>28</sub> H <sub>18</sub> O <sub>2</sub> ·2(C <sub>6</sub> H <sub>7</sub> N)
Molar ratio of host:guest	1:2	1:2	1:2	1:2
Molecular mass/g mol <sup>-1</sup>	544.62	572.68	572.68	572.68
Crystal symmetry	monoclinic	monoclinic	monoclinic	monoclinic
Space group	P2 <sub>1</sub> /n	P2 <sub>1</sub> /n	P2 <sub>1</sub> /n	C2/c
<i>a</i> /Å	9.1605(1)	8.7898(2)	8.8016(3)	22.2738(1)
<i>b</i> /Å	9.2707(3)	9.6027(2)	10.4056(3)	10.0706(2)
<i>c</i> /Å	18.0680(9)	18.0981(2)	17.2968(6)	16.8250(3)
$\alpha$ /°	90	90	90	90
$\beta$ /°	96.589(1)	95.880(1)	97.770(1)	122.876(2)
$\gamma$ /°	90	90	90	90
<i>Z</i>	2	2	2	4
<i>V</i> /Å <sup>3</sup>	1524.28(9)	1519.6(5)	1569.57(9)	3169.6(1)
<i>D</i> <sub>c</sub> /g cm <sup>-3</sup>	1.187	1.252	1.212	1.200
$\mu$ (MoK $\alpha$ )/mm <sup>-1</sup>	0.073	0.077	0.074	0.074
<i>F</i> (000)	572	604	604	1208
Temp. of collection/K	173	113	113	113
Range scanned, $\theta$ /°	2.5–27.9	2.4–27.9	2.4–27.9	2.2–27.8
Index ranges ( <i>h, k, l</i> )	-11/11; -11/9; -20/23	-11/11; -9/12; -23/23	-11/11; -13/13; -22/22	-29/29; -13/13; -21/22
No. reflections collected	9143	5583	7028	13342
No. unique reflections	3274	3615	3751	3739
	<i>R</i> <sub>int</sub> =0.054	<i>R</i> <sub>int</sub> =0.017	<i>R</i> <sub>int</sub> =0.040	<i>R</i> <sub>int</sub> =0.050
No. reflections with <i>I</i> >2 $\sigma$ ( <i>I</i> )	1351	2696	2389	2213
Data/parameters refined	3274/195	3615/204	3751/204	3739 / 205
Goodness of fit, <i>S</i>	0.95	1.04	1.00	1.00
Final <i>R</i> indices ( <i>I</i> >2 $\sigma$ ( <i>I</i> ))	<i>R</i> <sub>1</sub> =0.0514 <i>wR</i> <sub>2</sub> =0.1636	<i>R</i> <sub>1</sub> =0.0412 <i>wR</i> <sub>2</sub> =0.1059	<i>R</i> <sub>1</sub> =0.0468 <i>wR</i> <sub>2</sub> =0.1166	<i>R</i> <sub>1</sub> =0.0449 <i>wR</i> <sub>2</sub> =0.1225
Largest diff. peak and hole/e Å <sup>-3</sup>	-0.12 and 0.19	-0.22 and 0.28	-0.27 and 0.19	-0.15 and 0.15

jector, a FID detector, a Varian fused silica column (15 m length, 0.25 mm diameter) and a CP-8400 AutoSampler. The chromatograms obtained were recorded and analysed using the Galaxie GC WS software [13]. The method used for all the measurements was the following: injection volume: 1  $\mu\text{L}$ , injector temperature: 200°C, column temperature: 70°C, detector temperature: 250°C, carrier gas: helium (flow rate: 1.6 mL  $\text{min}^{-1}$ ).

Before each set of competition experiments, the GC analyser was calibrated by analysing the starting mixture of known mole fraction of the guests. The reproducibility was checked by repeating the measurements two to three times and made possible by the use of the autosampler, which ensured the injection of consistent amounts of sample.

## Results and discussion

### Structures

The compound WEB22·2(PYR) crystallizes in the space group  $P2_1/n$  with  $Z=2$ . The host molecule therefore lies on a centre of inversion at Wyckoff position b, with the guest in a general position. The structure is stabilized by (host) O–H $\cdots$ N (guest) hydrogen bonds with  $d\text{ O}\cdots\text{N}=2.783(3)\text{ \AA}$ , as shown in Fig. 1. The metrics of the hydrogen bond for this and the other compounds are displayed in Table 2.

The packing of the host molecules is such that they form channels parallel to [100] in which the guests are located. These are hour-glass shaped with maximum cross section of  $10.0\times 5.8\text{ \AA}$  and restricting to  $5.2\times 4.8\text{ \AA}$ . The packing with the host atoms in van der Waals radii representation and the guests omitted is shown in Fig. 2.

The structure of WEB22·2(2PIC) and WEB22·2(3PIC) are similar to that of WEB22·2(PYR), and are isostructural with respect to

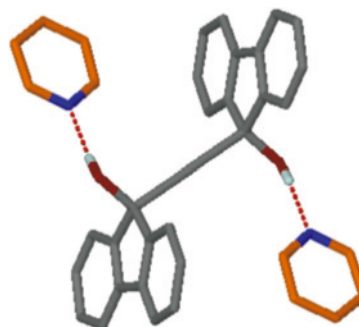


**Fig. 1** Hydrogen bond in the inclusion compound WEB22·2(PYR) with  $d\text{ O}\cdots\text{N}=2.783(3)\text{ \AA}$

the host molecules. The sizes of the channels are reported in Table 2.

The compound WEB22·2(4PIC) crystallizes in the space group  $C2/c$  with  $Z=4$ . The host molecules lie again in a centre of inversion at Wyckoff position b and the guests in general position. Although the unit cell parameters are different, there are similarities between this structure and that of the other three compounds. The host molecules pack with their major molecular axis parallel to [101], but the channels in the WEB22·2(4PIC) structure are now parallel to [001].

CCDC 629177 to – 629180 contains the supplementary crystallographic data for this paper. These data can be obtained free of charge via [www.ccdc.cam.ac.uk/data\\_request/cif](http://www.ccdc.cam.ac.uk/data_request/cif), by emailing [data\\_request@ccdc.cam.ac.uk](mailto:data_request@ccdc.cam.ac.uk), or by contacting The Cambridge Crystallographic Data Centre, 12, Union Road, Cambridge CB2 1EZ, UK; fax: +44 1223 336033.

### Selectivity

Competition experiments are employed to measure the selectivity of a host for a given guest in a mixture of guests. In general, four kinds of selectivity curves arise as shown in Fig. 3.  $X_A$  is the mole fraction of

**Table 2** Metrics of the hydrogen bonds and of the channels in the inclusion compounds of WEB22

	WEB22·2(PYR)	WEB22·2(2PIC)	WEB22·2(3PIC)	WEB22·2(4PIC)
Metrics of the hydrogen bonds				
Donor–H (Host)	O <sub>(1)</sub> –H <sub>(1)</sub>	O <sub>(1)</sub> –H <sub>(1)</sub>	O <sub>(1)</sub> –H <sub>(1)</sub>	O <sub>(1)</sub> –H <sub>(1)</sub>
Acceptor (Guest)	N <sub>(1G)</sub>	N <sub>(1G)</sub>	N <sub>(1G)</sub>	N <sub>(1G)</sub>
$d\text{ D–H (Å)}$	0.89(3)	0.97(2)	0.94(2)	0.94(2)
$d\text{ H}\cdots\text{A (Å)}$	1.91(3)	1.82(2)	1.82(2)	1.81(2)
$d\text{ D}\cdots\text{A (Å)}$	2.783(3)	2.777(2)	2.754(2)	2.747(2)
Angle (°) (D–H $\cdots$ A)	164(3)	169(2)	172(2)	174(2)
Metrics of the channels				
Maximum aperture (Å $\times$ Å)	10.0 $\times$ 5.8	9.2 $\times$ 6.2	9.6 $\times$ 6.5	7.5 $\times$ 7.5
Minimum aperture (Å $\times$ Å)	5.2 $\times$ 4.8	5.1 $\times$ 4.8	6.2 $\times$ 4.1	7.2 $\times$ 5.1

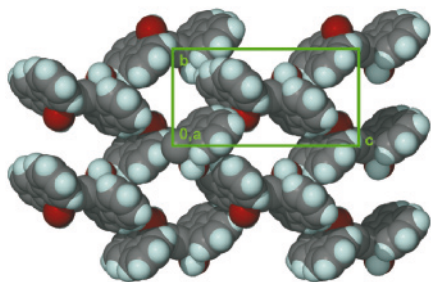


**Fig. 2** Packing of WEB22·2(PYR) with WEB22 represented in van der Waals radii, the pyridine molecules being omitted to show the channels

guest A in the liquid mixture, and  $Z_A$  is that of the guest entrapped in the crystal [14].

Curve *a* occurs when A is preferentially enclathrated over the whole concentration range. Curve *b* lies close to the diagonal line of unit slope and shows very poor selectivity. Curve *c* results when the selectivity is concentration dependent with A and B being preferentially enclathrated when they are in high concentration in the mother liquor. Curve *d* exhibits ‘inverse concentration’ dependence, in that the host enclathrates the guest of lower mole fraction in the mother liquor. This is counter intuitive and unusual, but has been shown to occur in the selectivity of 3-picoline

vs. 4-picoline by a resorcinarene host [15]. The method can be extended to the analysis of the competition for three guests simultaneously, in which case the results are displayed in an equilateral triangle in which each apex represents a pure guest.

The selectivity results are displayed in Figs 4a and b. In Figure 4a, we note that 4-picoline is preferentially enclathrated over pyridine over the complete range of solutions. Very poor selectivities occur between 4-picoline and 2-picoline and between 2-picoline and pyridine. In the three-component system comprising pyridine, 4-picoline and 2-picoline, the starting compositions are shown by the points in the inner triangle, which drift towards 2-picoline upon enclathration.

Figure 4b shows that in the cases of pyridine, 2-picoline and 3-picoline, the two-component competition experiments all display concentration dependent selectivities, while the three-component experiment shows virtually no selectivity upon enclathration.

#### Thermal analysis

The thermal analysis results are shown in Fig. 5. The desorption of WEB22·2(PYR), shown in Fig. 5a, displays two steps for the mass loss and an endotherm A

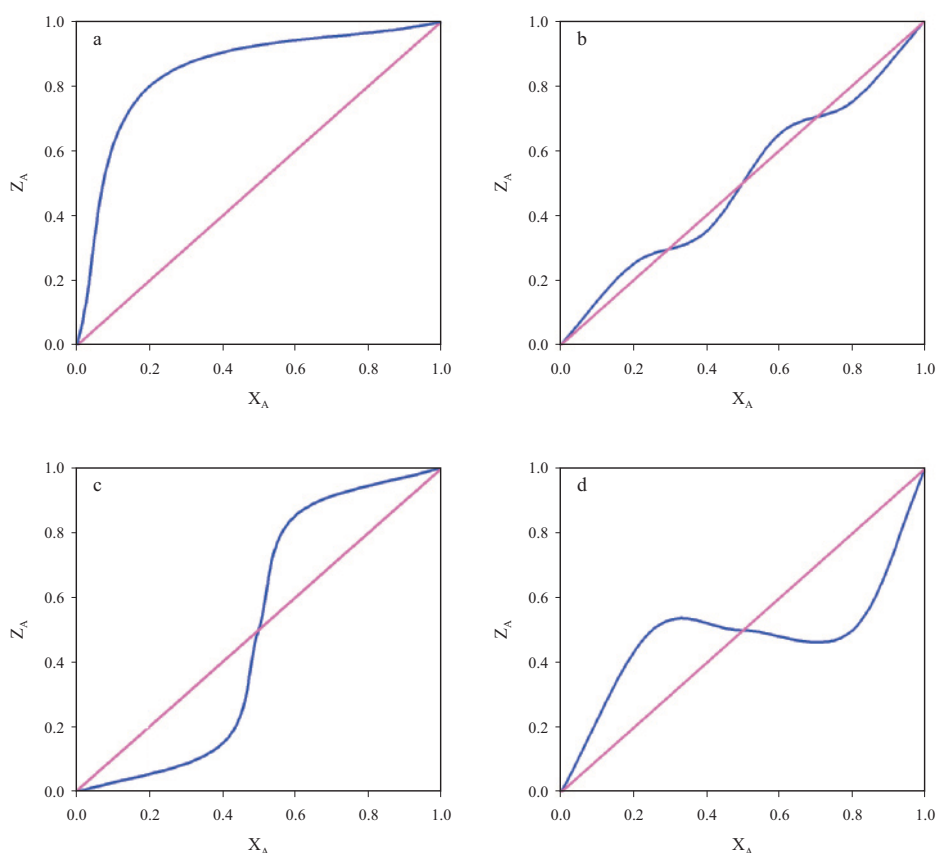


**Fig. 3** Selectivity curves obtained from a 2-component competition experiment

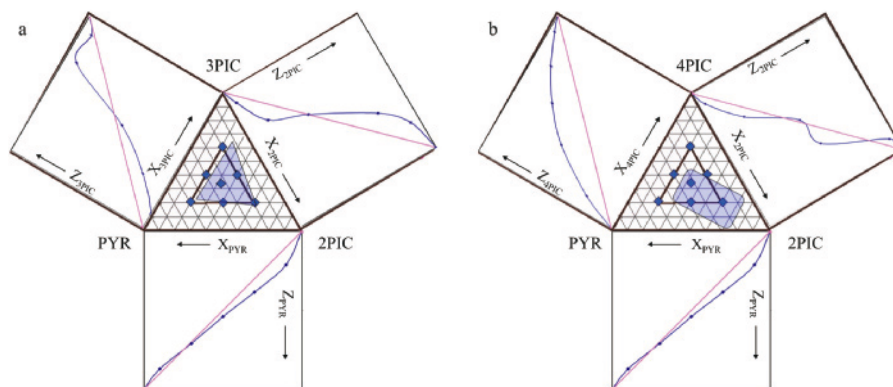


**Fig. 4** a – Competition experiment of WEB22 with pyridine, 2-picoline and 3-picoline and b – competition experiment of WEB22 with pyridine, 2-picoline and 4-picoline

corresponding to the guest loss, followed by an endotherm B attributed to the melt of the host compound. Similar patterns are observed for the other three compounds, as shown in Figs 5b–d. The results of the analyses are given in Table 3.

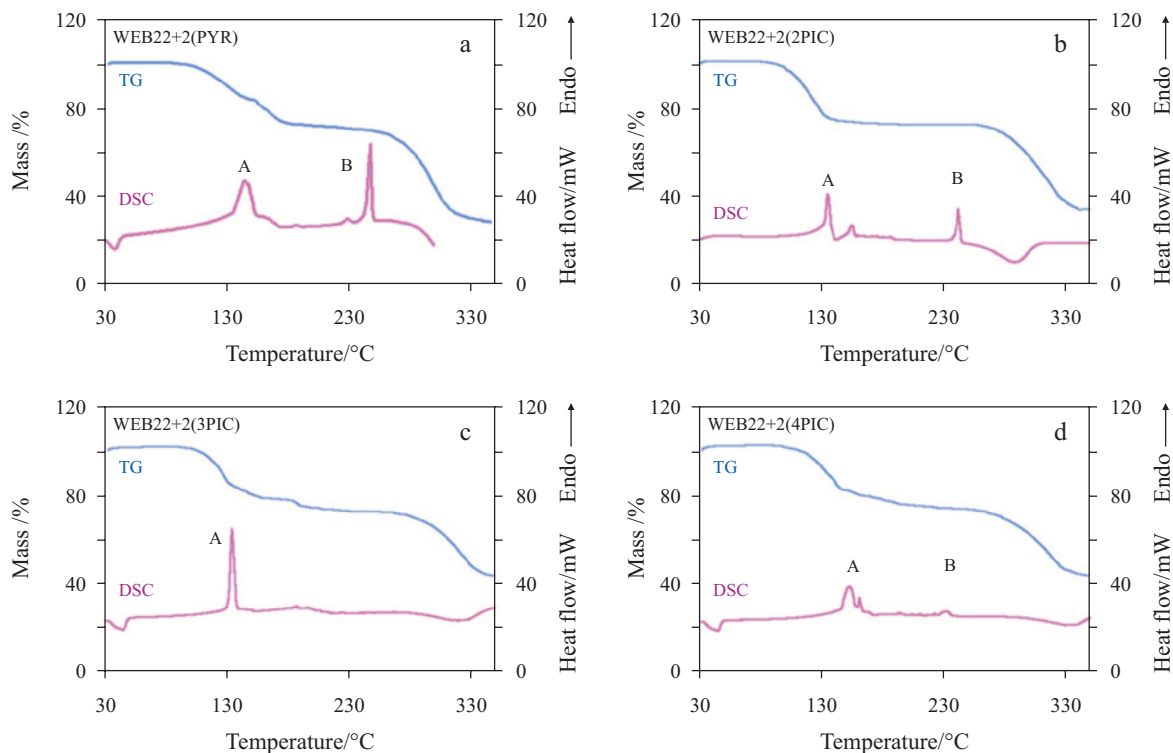
*Kinetics of desorption*

The thermal gravimetry curve for the desorption of the WEB22·2(2PIC) compound was the one which displayed the smoothest, single mass-loss step. We therefore chose this compound in order to analyse the kinetics of desorption. The  $\alpha$ -time curves shown in Fig. 6 were deceleratory and fitted the Avrami–Erofe’ev, A2 law:

$$[\ln(1-\alpha)]^{1/2} = kt$$

The semilogarithmic plot of  $\ln k$  vs.  $1/T$  yielded a satisfactory straight line (Fig. 7) corresponding to an activation energy  $E_a = 111(7) \text{ kJ mol}^{-1}$ .

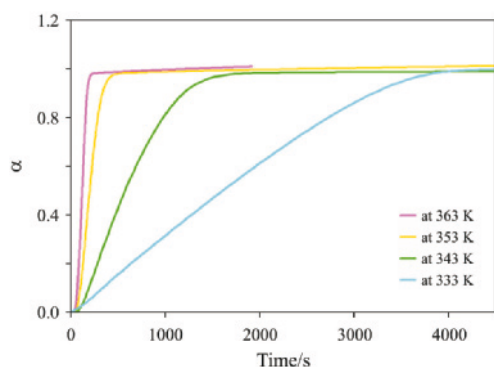
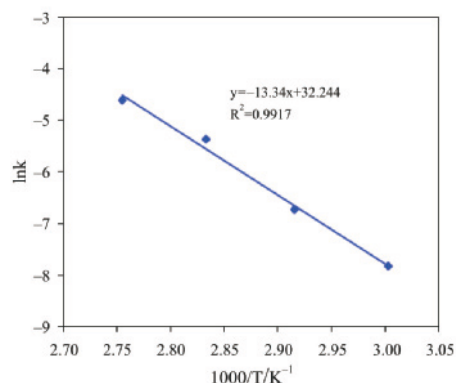
This value is similar to those obtained for other hydroxyl hosts: in the inclusion compound formed between 9-(3-methoxyphenyl)-9*H*-xanthen-9-ol and aniline, the desorption is governed by the contracting area model R2, with  $E_a = 108(8) \text{ kJ mol}^{-1}$  [16], while in the related compound 9-(1-naphthyl)-9*H*-xanthen-9-ol with dioxane as guest, the desorption kinetics fitted the Avrami A4 law and yielded an activation energy of  $111(2) \text{ kJ mol}^{-1}$  [17].



**Fig. 5** TG and DSC traces of a – WEB22·2(PYR), b – WEB22·2(2PIC), c – WEB22·2(3PIC) and d – WEB22·2(4PIC)

**Table 3** Results of the thermal analyses

	WEB22-2PYR	WEB22-2(2PIC)	WEB22-2(3PIC)	WEB22-2(4PIC)
H:G ratio	1:2	1:2	1:2	1:2
TG %calc	29.1	32.6	32.6	32.6
%obs	28.4	27.9	29.4	28.5
DSC $T_{on}$ peak A	133	132	132	145
$T_{on}$ peak B	244	240	–	227
$T_b$	115	128	144	145


**Fig. 6** The  $\alpha$ -time curves for the desorption of the WEB22-2(2PIC) compound

**Fig. 7** The semilogarithmic plot of  $\ln k$  vs.  $1/T$  for the desorption of WEB22-2(2PIC) compound

## Conclusions

The structure of the inclusion compound 9,9'-(ethyne-1,2-diyl)bis(fluoren-9-ol) with pyridine and the isomers of picoline are essentially similar, with the guests lying in undulating channels, and stabilised by host-guest hydrogen bonds. This structural similarity is reflected in their selectivity and thermal behaviour, in that there is poor discrimination of any guest upon enclathration. The activation energy for the desorption reaction of the 2-picoline compound is similar to that found in similar clathrates.

## References

- 1 E. Weber, *Comprehensive Supramolecular Chemistry*, D. D. Mac Nicol, F. Toda and R. Bishop, Eds, Elsevier, Oxford, 6 (1991) 535.
- 2 E. Weber, *Inclusion Compounds*, J. L. Atwood, J. E. D. Davies and D. D. Mac Nicol, Eds, Oxford University Press, Oxford, 4 (1991) 188.
- 3 E. Weber, S. Nitsche, A. Wierig and I. Csöreg, *Eur. J. Org. Chem.*, (2002) 856.
- 4 F. Toda, *Topics in Current Chemistry*, Vol. 40, Molecular Inclusion and Molecular Recognition, E. Weber, Ed., Springer-Verlag, Berlin 1987, p. 43.
- 5 M. R. Caira, L. R. Nassimbeni, F. Toda and D. Vujovic, *J. Chem. Soc. Perkin Trans.*, 2 (2001) 2119.
- 6 COLLECT, Data Collection Software, Nonius, Delft, The Netherlands 1998.
- 7 Z. Otwinowski and W. Minor, *Methods in Enzymology: Macromolecular Crystallography*, C. W. Carter Jr. and R. M. Sweet, Eds, Academic Press, New York 1997; part A, Vol. 276, 307.
- 8 G. M. Sheldrick, SHELX-86: Crystallographic Computing; G. M. Sheldrick, C. Kruger and R. Goddard, Eds, Oxford University Press, Oxford, UK, 3 (1985) 175.
- 9 G. M. Sheldrick, SHELX-97: Program for Crystal Structure Refinement, University Of Göttingen, Germany 1997.
- 10 L. J. J. Barbour, *Supramol. Chem.*, 1 (2001) 189.
- 11 J. L. Atwood and L. J. Barbour, *Cryst. Growth Des.*, 3 (2003) 3.
- 12 M. E. Brown, *Introduction to Thermal Analysis*, Chapman and Hall, London 1988.
- 13 Galaxie Chromatography Workstation, Version 1.7.403.22, Varian, Inc. 2002.
- 14 L. R. Nassimbeni, *Separations and Reactions in Organic Supramolecular Chemistry*, F. Toda and R. Bishop, Eds, Wiley, Chichester 2004, Chapter 5.
- 15 M. R. Caira, T. Le Roex and L. R. Nassimbeni, *Cryst. Eng. Comm.*, 8 (2006) 275.
- 16 A. Jacobs, L. R. Nassimbeni and J. H. Taljaard, *Cryst. Eng. Comm.*, 7 (2005) 731.
- 17 A. Jacobs, L. R. Nassimbeni and J. H. Taljaard, *Acta Cryst.*, C60 (2004) 668.

DOI: 10.1007/s10973-007-8474-0